

Journal of Robotics and Mechanical Engineering Research

Performance Analysis of Cold Sections of High BYPASS Ratio Turbofan Aeroengine

Ahmed F. El-sayed*, Mohamed S. Emeara and Mohamed K. Fayed

Department of Mechanical Power, Engineering College, Zagazig University, Egypt

***Corresponding author:** Ahmed F. El-sayed, Department of Mechanical Power, Engineering College, Zagazig University, Zagazig 44519, Egypt; E mail: dr_ahmedhelal@yahoo.com

Article Type: Case Report, **Submission Date:** 04 August 2017, **Accepted Date:** 28 August 2017, **Published Date:** 31 October 2017.

Citation: Ahmed F. El-sayed, Mohamed S. Emeara and Mohamed K. Fayed (2017) Performance Analysis of Cold Sections of High BYPASS Ratio Turbofan Aeroengine. J Robot Mech Eng Resr 2(1): 18-27. doi: <https://doi.org/10.24218/jrmer.2017.23>.

Copyright: © 2017 Ahmed F. El-sayed, et al. This is an open-access article distributed under the terms of the Creative Commons Attribution License, which permits unrestricted use, distribution, and reproduction in any medium, provided the original author and source are credited.

Abstract

The turbofan engine had many developments in the past 60 years and becomes the common power plant employed in both civil airliners and military aircrafts. It combines the advantages of both of turboprop engines (high propulsive efficiency and thrust) and turbojet engines (high flight speed and altitude). To cope with the needs of high thrust forces that propel wide body airliner and increase of their payload and range as well as enlarging maneuver capabilities of military aircrafts, successive developments of turbofan engines are needed. These developments in turbofan design have endeavors of larger thrust force, low noise and emission as well as better fuel economy. These goals were achieved by increasing of the bypass ratio (BR), fan pressure ratio (FPR), overall pressure ratio (OPR), turbine inlet temperature (TIT) as well as using new materials, production and cooling techniques for both turbines and combustion chamber such modifications led to improvements in thermal, propulsive and overall efficiencies, decreases in thrust specific fuel consumption (TSFC) and increase the specific thrust. This paper presents a parametric study and design point selection of the cold sections of high bypass ratio turbofan engine (close to GEnx-1B-70). Cold sections include the intake, the fan, and the compressor. This engine is one of the products of GE Aviation Company. Performance analysis is performed using MATLAB program code for both taking-off and cruise conditions.

Introduction

The bypass turbofan GE design was conceived to improve the fuel efficiency for commercial aircraft. An additional component – the fan – is installed at the inlet of the engine to increase the amount of air flowing through the engine. However, part of the inlet airflow is not directed toward the compressor, combustor, and turbine, but is rather bypassed through a duct, which ends in a nozzle. Since air leaves the nozzle at a speed which is higher than the intake velocity, thrust is produced by momentum

exchange with the airframe. The flow which is not bypassed undergoes the processes mentioned in the turbojet section, producing part of the total thrust. Note that the thrust generated by the bypass flow does not require the burning of fuel, but some mechanical work must be derived from a turbine to drive the fan. Turbofans can be classified according to number of spools or whether the two jets are mixed among other criteria. From the first turbo supercharger to the world's most powerful commercial jet engine, GE's history of powering aircraft spans nearly a century of innovation GE Aviation is a world-leading provider of commercial and military jet engines and components as well as integrated digital, electric power, and mechanical systems for aircraft. GE Aviation also has a global service network to support these offerings Technological excellence, supported by continued investments in research and development, has been the foundation of GE Aviation's growth and helps to ensure quality products for customers well into the future.

In the present paper the components of (GEnX-1B70) turbine engine will be discussed as: 1- Intake, 2- Fan, 3- Compressor, 4- Combustion Chamber, 5- Turbine, and 6- Nozzle. They will be discussed briefly in the following sections.

Engine intake compatibility covers the mutual dependencies between the aircraft intake and the gas turbine. Besides exhibiting optimal performance it is of utmost importance that stable propulsion operation in the whole flight envelope of a jet aircraft is ensured. In this chapter the effects of intake flow distortions on the operation conditions of engine components and the whole gas turbine will be described there are three types of intakes subsonic or supersonic and hypersonic note (GEnx-1B-70) subsonic intake.

Fans have progressed through the years but here we discuss two important fans; this of the GE90 engine and that of the GEnX engine there are fan materials titanium or bi-metals and composite.

In the gas turbine engine, compression of the air before expansion through the turbine is effected by one of two basic types of compressor, one giving centrifugal flow and the other axial flow. Both types are driven by the engine turbine and are usually coupled direct to the turbine shaft. An axial flow compressor consists of one or more rotor assemblies that carry blades of airfoil section. These assemblies are mounted between bearings in the casings which incorporate the stator vanes. The compressor is a multi-stage unit as the amount of pressure increase by each stage is small; a stage consists of a row of rotating blades followed by a row of stator vanes. Where several stages of compression operate in series on one shaft it becomes necessary to vary the stator vane angle to enable the compressor to operate effectively at speeds below the design condition. As the pressure ratio is increased the incorporation of variable stator vanes ensures that the airflow is directed onto the succeeding stage of rotor blades at an acceptable angle, ref. para. 30, Airflow Control.

The engine close to GEnx-1B-70 by General Electric Company is the present case study. Table 1 shows the main data of the engine. Also Figure 1 shows the number of each station considered in the present study of the present engine. The engine is suitable to be installed on the Boeing 787-8 Dreamliner. The engine is two (twin) spool and high by-pass ratio (HBPR) turbofan engine. The engine consist of single fan, 4 low-pressure compressors (LPC), 10 high-pressure compressors (HPC), combustion chamber (CC), 2 high-pressure turbines (HPT), 7 low-pressure turbines (LPT), and nozzle. The overall performance of the engine will calculated and discussed for both taking-off and cruise conditions.

Table 1: Turbofan Engine GEnX-1B-70 specifications

Title	Sym-bol	Value	Unit
Width	-	3,533.1	mm
Height	-	3,484.9	mm
Overall Length	-	4,950.5	mm
Intake/Fan Diameter	D_f	2.82	m
Max. Take-off Thrust (5 min.)	T_{max-TO}	321.735	kN
Fan speed at Take-off Thrust (5 min.)	N_{f-TO}	2,401	rpm
Max. continuous thrust	T_{max-C}	295.8	KN
Fan speed (max. continuous thrust)	N_{f-C}	2,319	rpm
Pressure Ratio of High-Pressure Compressor	π_{HPC}	23	-
Overall Pressure Ratio (at max. power)	OPR_{Max}	43.5	-
Fuel flow rate(Take-off)	\dot{m}_{f-TO}	2.037	rpm
Fuel flow rate (Cruise)	$\dot{m}_{f-Cruise}$	2.494	m/s
Bypass ratio	β	9.1	-
Total air mass flow rate (Take-off)	\dot{m}_{a-TO}	1155.43	kg/s
Bypass air flow rate	\dot{m}_{a-BP}	1041.03	kg/s
Core air flow rate	\dot{m}_a	114.399	kg/s
Fuel heating value	Q_R	42555.066	kJ/kg
Air bleed % (7 Stages)	-	3.3	-

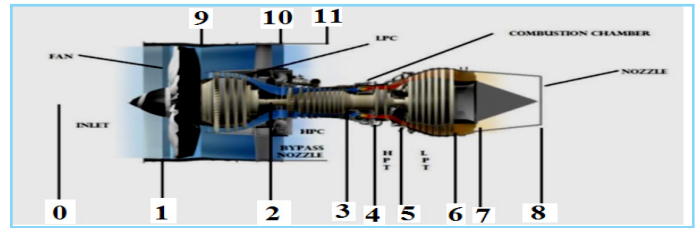


Figure 1: GEnx-1B70 modules and Stations numbering

Overall Engine data at Taking-off and Cruise

The considered data which are assumed according to the published references and which is valid with the engine specifications are illustrated in Table 2.

Table 2: Assumed Engine Modules Efficiencies

Intake	Fan	HPC	LPC		Fan nozzle
0.97	0.91	0.91	0.91	0.99	0.96

The overall engine parameters are calculated at taking-off condition in Table 3 and the pressure (kPa) and the temperature (K) are calculated and illustrated in Table 4.

Table 3: Calculated overall Engine Data at Taking-off condition

Title	Value	Unit
π_{intake}	1.0	-
π_{Fan}	1.5	-
π_{LPC}	1.3	-
π_{HPC}	22.3	-
TIT	1790	K
\dot{m}_a	1155.43	kg/s
\dot{m}_f	3.21	kg/s
Thrust force	320.48	kN
Specific Thrust	0.28	kg/S.KN
TSFC	0.01	kg/S.KN
Hot Jet velocity (The turbine nozzle is not choked)	401.921	m/s
Cold Jet velocity (The fan Nozzleis not choked)	262.67	m/s

The calculated data for the overall engine performance is seen in Table 5. The pressure (kPa) and the temperature (K) at each station of the engine (see Figure1) are calculated and illustrated in Table 6.

Intake Design Calculations

The following equations are the governing equations for both the taking-off and the cruise condition. Also, Figure 2 and Figure 3 are the calculated intake dimensions according to taking-off and cruise condition, respectively.

According to Take-off condition

For Core section

Table 4: Calculated Pressure and Temperature at Engine-station at Taking-off condition

Station no.	Total Temperature (K)	Static Temperature (K)	Total Pressure (kPa)	Static Pressure (kPa)
1	Ta =288.00	-	Pa=101.325	-
2	354.83	-	197.58375	-
Bleed station	744.64	-	2149.58	-
3	911.70	-	4407.6375	-
4	1790.00	-	4319.48475	-
5	1212.70	-	758.41206	-
6	838.39	-	146.05499	-
7	838.39	-	146.05499	-
8	-	838.39	-	146.05499
9	326.87	-	151.98750	-
10	326.87	-	151.98750	-
11	-	326.87	-	151.98750

Table 5: Calculated overall Engine Data at Cruise Condition

Title	Value	Unite
π_{intake}	1.0	-
π_{Fan}	1.4	-
π_{LPC}	1.3	-
π_{HPC}	23.9	-
TIT	1690	k
m'_a	1155.43	kg/s
m'_F	2.82	kg/s
Thrust force	293.25	kN
Specific Thrust	0.25	kN-s/kg
TSFC	0.01	kg/s.kN
Cold Jet velocity (The fan Nozzleis not choaked)	237.88	m/s

Table 6: Calculated Pressure and Temperature at Engine-station at CruiseCondition

Station NO.	Total Temperature (K)	Total Pressure (kPa)
1	288.00	101.325
2	347.30	184.4115
Bleed station	741.75	2122.99
3	910.80	4407.6375
4	1690.00	4319.48475
5	1104.16	642.29973
6	791.85	146.12272
7	791.85	146.12272
8	791.85	146.12272
9	319.94	141.855
10	319.94	141.855
11	319.94	141.855

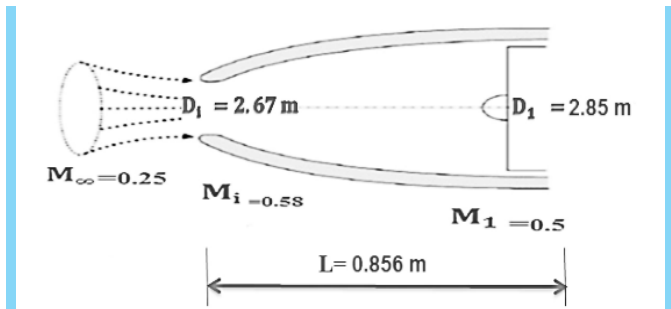


Figure 2: Intake dimensions according to take-off calculations

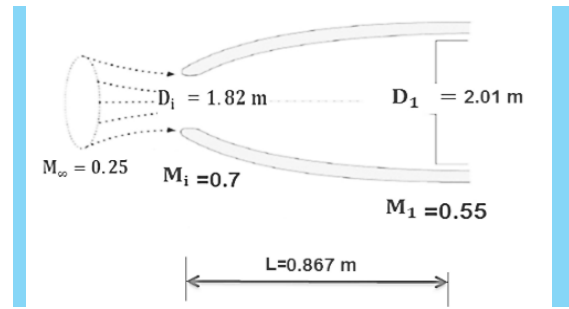


Figure 3: Intake dimensions according to cruise calculations

$$A_i = 5.604 \text{ m}^2$$

$$A_i = \frac{\delta}{4} * D^2$$

$$\therefore D_i = 2.67 \text{ m}$$

At fan section

$$A_i = 6.19 \text{ m}^2$$

$$A_i = \frac{\delta}{4} * [D^2 - 0.5^2]$$

$$\therefore D_i = 2.85 \text{ m}$$

$$\therefore P_i = 83.27 \text{ kpa}$$

$$\therefore T_i = 279.18 \text{ K}$$

$$L = 0.856 \text{ m}$$

According to Cruise condition

At Core section

$$A_i = 2.6 \text{ m}^2$$

$$A_i = \frac{\delta}{4} * D^2$$

$$\therefore D_i = 1.82 \text{ m}$$

At fan section

$$A_i = 2.98 \text{ m}^2$$

$$A_i = \frac{\delta}{4} * [D^2 - 0.5^2]$$

$$\therefore D_i = 2.01 \text{ m}$$

$$\therefore P_i = 80.42 \text{ kpa}$$

$$\therefore T_i = 276.42 \text{ K}$$

$$\therefore L = 0.867 \text{ m}$$

By comparing the two case of calculations, the cruise case is satisfied with take-off condition. Then, the cruise calculation is valid and considered as the final engine dimensions.

Fan Design Calculations

Bypass ratio (B):9.1

Material: Titanium

Fan Diameter: 2.82 M

Design Procedures

a- Rotational speed and axial velocity

b- Air angles and Velocity triangles at mean

c- Radial variation from hub to tip

d- Chord and Torque distribution over the blade

e- Fan blading and Cascade design

Rotational and Axial Velocities

Known Parameters

- 1- Hub to tip ratio
- 2- Tip diameter
- 3- Air mass flow rate
- 4- Total temperature and pressure before and after the fan

Assumed Parameters

- 1- Tip Mach number (1.5)
- 2- Flow is axial at inlet

Calculated Parameters

1-axial velocity

$$\dot{m}_a = \frac{P_i}{RT_i} AC_a$$

$$T_i = \text{TOI} - \frac{C_a^2}{2 C_p}, P_i = P_{01} \left(1 - \frac{C_a^2}{2 T_{01} * C_p} \right)^{3.5}$$

From the above equations the only unknown is C_a

2-rotational velocity:

$$\therefore M_{\text{rel}})_t = \frac{W_{it}}{\sqrt{\gamma RT_i}}$$

$$\therefore W_t^2 = U_t^2 + Ca^2$$

Air angles & Velocity triangles

At mean section

Known:

- 1- U_m
- 2- Ca
- 3- α_1
- 4- ΔT_o

$$\beta_1 | _m = \tan^{-1} \left(\frac{U_m}{Ca} \right) \tan^{-1}$$

$$\Delta T_o = \frac{\lambda U_m C_p (\tan \beta_1 - \tan \beta_2)}{C_p}$$

$$\frac{U_m}{C_a} = \tan(\beta_2) + \tan(\alpha_2)$$

$$W_1^2 = U_1^2 + C_{a1}^2$$

$$C_2 = \frac{C_{a1}}{\cos(\alpha_2)}$$

$$W_2 = \frac{C_{a1}}{\cos(\beta_2)}$$

Air angles & Velocity triangles

At mean section

Figure 4 and Figure 5 show the velocity triangles for the airfoil at tip section and mean section, respectively. Figure 6 shows velocity triangle for airfoil at hub section of the fan blade.

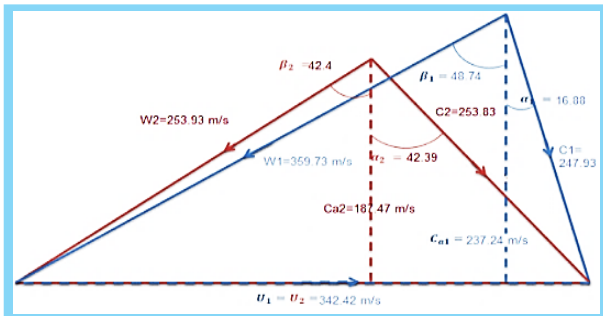


Figure 4: Velocity triangle for airfoil at tip section of for the fan by free vortex method

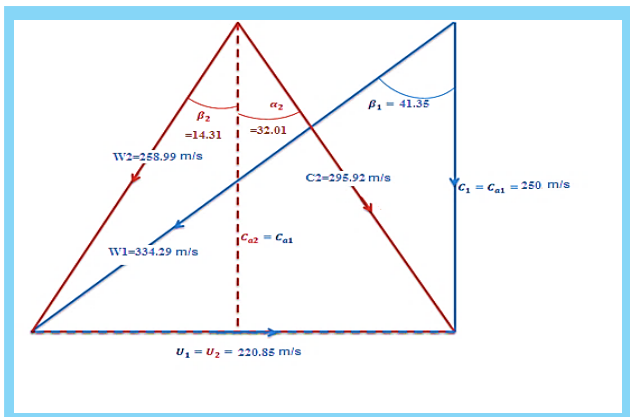


Figure 5: Velocity triangle for airfoil at mean section of the fan blade

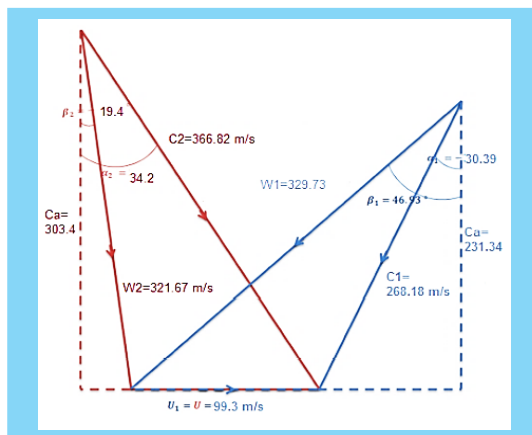


Figure 6: Velocity triangle for airfoil at hub section of the fan blade

Radial variation from hub to tip

Table 7 shows the data of radial variation from hub to tip.

Velocity triangle:-

At Tip section

Chord and Thrust distribution over the blade

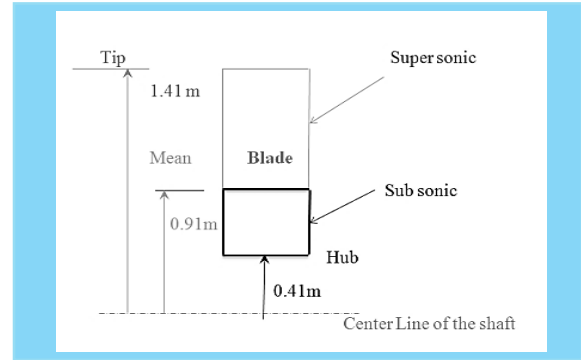


Figure 7: Dimensions of blade

The Chord distribution is assumed and then checked by comparing the fan torque to the torque from each section “20 section” where:

$$1- \text{Total torque : } T = \frac{P}{\omega} = 185,498.8 \text{ N.M}$$

2- Torque from each section:

$$d\tau = \frac{\rho C_L^2 c Z C_r r dr}{2 \cos^2 \beta_m} * \frac{\cos(\beta_m - \gamma)}{\cos \gamma}$$

C_L and C_D are based on a NACA-65 series report for various Mach numbers and angles of attack. Table 8 shows Chord and Thrust distribution over the blade.

Fan Blading and Cascade Design

The blade twist angle

Twist angle at inlet =

$$\beta'_{it} - \beta'_{ih} = 48.74^\circ - 45.44^\circ = 3.3^\circ$$

$$\text{Twist angle at exit} = \beta'_{2t} - \beta'_{2h} = 32.42^\circ - (-29.4^\circ) = 61.82^\circ$$

The spacing between the fan blades

$$S = \frac{2\pi * r_m}{n} = \frac{2\pi * 0.91}{18} = 0.32 \text{ m}$$

$$\therefore S = 0.32 \text{ m}$$

Airfoil

Root : subsonic airfoil

Tip: supersonic airfoil

sharp edges at

leading edge/trailing edge

Figure 7 shows the blade dimensions and Figure 8 shows the blade which is drawing by solidworks software.

Table 8: Chord and Thrust distribution over the blade

Section	m/s	Chord (mm)	M_{rel}	C_l	rm	d_t
1	250.00	495	1.1118	0.616456	0.410	2057.42
2	235.82	500	1.121	0.616452	0.441	2150.42
3	246.93	505	1.102	0.615	0.472	2591.75
4	250.33	510	1.113	0.614	0.503	2919.93
5	256.91	515	1.124	0.613	0.534	4306.21
6	269.25	520	1.138	0.612	0.565	5118.66
7	278.90	525	1.155	0.610	0.596	6115.43
8	290.32	530	1.720	0.609	0.627	5016.51
9	302.22	535	1.180	0.608	0.658	6093.03
10	312.80	540	1.210	0.605	0.689	6584.62
11	324.61	545	1.220	0.600	0.720	7165.25
12	333.83	550	1.240	0.598	0.751	8419.69
13	350.64	555	1.260	0.594	0.781	9468.20
14	372.70	560	1.280	0.590	0.813	12226.96
15	398.67	565	1.300	0.588	0.844	12243.96
16	413.90	570	1.320	0.585	0.875	16425.79
17	425.83	575	1.340	0.582	0.906	174843.96
18	433.73	580	1.360	0.579	0.937	19187.05
19	445.68	585	1.376	0.578	0.968	20646.75
20	450.25	590	1.380	0.576	0.999	21364.78
Sum.						185,529.92



Figure 8: Mechanical drawing of Aero-Engine fan according to dimensions calculated in the present design by using solid-works software

The Axial Compressor

Calculation of ω for the compressor

Assume:-

- 1- hub-to-tip ratio (0.8)
- 2- C_a (128.5 m/sec.)
- 3- M_1 tip rel(0.95)

Known:-

- 1- T_1
- 2- P_1

$$M_{(rel)_t} = \frac{W_t}{\sqrt{\gamma RT_1}}$$

$$\dot{m}a = \frac{P_1}{RT_1} A C_a$$

$$A = \pi (r_t^2 - r_h^2)$$

Knowing , hub to tip ratio $\zeta = \frac{r_h}{r_t}$

$$W_1^2 = U_1^2 + C_{a1}^2$$

$$\omega = \frac{ut}{rt}$$

Then,

$$N = 2,319 \text{ rpm}$$

Compressor Design

L.P.C. Design

Assumptions

$$\xi = 0.6 : 0.8 (0.8)$$

$$C_1 = 120 : 128.5 \text{m/s (128.5 m/s)}$$

Given

$$n.o.stage = 4$$

$$N = 2,319 \text{ rpm}$$

$$T_{01} = 319,94 \text{K}$$

$$P_{01} = 141.855 \text{ kpa}$$

$$T_{02} = 347.30K$$

$$P_{02} = 184.4115 K pa$$

$$So \Delta T_{0s} = 6.84k$$

$$C_p = 1005 KJ/kg.K$$

$$\gamma = 1.4$$

$$R = 287$$

$$M_a = 114.399 Kg/s$$

By: Using Design method" first power

Table 9 shows Calculated parameters for LPC from 1st to 4th stage. Table 10 shows also the calculated parameters from the 5th stage to the 14th final stage.

Table 9: Calculated parameters for LPC from 1st to 4th stage

stage	η_s	λ	r_t (m)	r_m (m)	r_h (m)	ΔT_{0s}	π_s
	0.91	0.98	0.398	0.304	0.211	40.25	1.43
	0.91	0.93	0.376	0.304	0.233	40.25	1.38
	0.91	0.88	0.362	0.304	0.248	40.25	1.34
	0.91	0.83	0.351	0.304	0.259	40.25	1.31

Table 10: Calculated parameters for HPC from 5th to 14th stage

stage	η_s	λ	r_t (m)	r_m (m)	r_h (m)	ΔT_{0s}	π_s
-	-	-	m	m	m	K	-
	0.91	0.83	0.342	0.304	0.267	40.25	1.28
	0.91	0.83	0.336	0.304	0.274	40.25	1.26
	0.91	0.83	0.357	0.304	0.279	40.25	1.24
	0.91	0.83	0.331	0.304	0.282	40.25	1.23
	0.91	0.83	0.324	0.304	0.285	40.25	1.22
	0.91	0.83	0.321	0.304	0.288	40.25	1.20
	0.91	0.83	0.319	0.304	0.290	40.25	1.19
	0.91	0.83	0.318	0.304	0.292	40.25	1.18
	0.91	0.83	0.316	0.304	0.293	40.25	1.17
	0.91	0.83	0.315	0.304	0.294	40.25	1.16

Blade Design

Cascade measurements

In order to obtain information on the effect of different blade designs on air flow angles, pressure losses and energy transfer across blade rows, one must resort to cascade wind tunnels and cascade theory. Experimentation here is performed to ensure that the blade row satisfies its objectives. The first objective is to turn air through the required angles ($\beta_1 - \beta_2$) for rotor and ($\alpha_3 - \alpha_2$) for stator, with the angle ($\beta_1 - \beta_2$) as a maximum as possible to maximize the stage pressure ratio. The second objective is to achieve the diffusing process with optimum efficiency, i.e., with minimum loss of stagnation pressure.

Calculation of no. of blades

We determine the number of blade at all stage and the chord length at all radii for all station. Details: For rotor we use β_1 & β_2 and for stator we use α_2 & α_3 . Table 11 shows the calculated number of blades of each stage for LPC.

Table 11: Calculated Number of blades of each stage for LPC

stage	r_t (m)	r_h (m)	H (m)	C	S/C	S	N
	0.398	0.211	0.187	0.0623	2.2	0.137	14
	0.376	0.233	0.143	0.047	2	0.094	20
	0.362	0.248	0.114	0.038	1.8	0.068	28
	0.351	0.259	0.092	0.031	1.8	0.056	34

For Rotor:

At mean section

$$\epsilon^* = \beta_1 - \beta_2 \text{ We get } s/c$$

We assume,

$$C = h/3 \text{ for low pressure compressor}$$

Then,

$S = (S/C) * C$ (Equ.16) No. of blade = $(2\pi * r_m) / S$ (Equ.17) From experience for rotor number of Blade is odd and for stator is even to avoid numbers with common multiples for the blades in successive rows to reduce the likelihood of introducing resonant forcing frequencies.

Where:

- Aspect ratio (h/c) is defined as hight divided by vane or blade chord.

- C The chord.

- S the space between two blades.

Table 11 shows Calculated Number of blades of each stage for LPC.

For Stator:

At mean section

$$\epsilon^* = \Delta \alpha \text{ We get } s/c$$

successive rows to reduce the likelihood of introducing resonant forcing frequencies.

Where:

$$T_s = T_{03} - \frac{C_a^2}{2C_p}$$

$$P_3 = P_{03} \left(\frac{T_3}{T_{03}} \right)^{\frac{\gamma}{\gamma-1}}$$

$$\rho_3 = \frac{P_3}{R * T_3}$$

$$M_{Tot.} = \rho_3 * A * C_{a3}$$

$$A = \frac{M_{Tot.}}{\rho_3 * C_{a3}}$$

$$A = \pi * r_m * h_s$$

$$h_s = \frac{A}{2\pi * r_m}$$

We assume,

C= h/3 for low pressure compressor

Then,

$$S=(S/C)*C$$

No. of blade = $(2\pi * r_m)/S$ From experience for rotor number of blade is odd and for stator is even to avoid numbers with common multiples for the blades.

- Aspect ratio (h/c) is defined as height divided by vane or blade chord.

- C The chord.

- S the space between two blades.

H.P.C. Design

Assumptions

$$\xi = 0.4 : 0.8 (0.53)$$

$$C1 = 150 : 200 \text{m/s} (200 \text{ m/s})$$

Given

$$\text{no. of stage} = 10$$

$$N = 11377 \text{ rpm}$$

$$T_{01} = 347.3 \text{K}$$

$$P_{01} = 184.4 \text{ kpa}$$

$$P_{0n} = 4407.6 \text{ K pa}$$

$$\text{So } \Delta T_{0s} = 40.25 \text{k}$$

$$C_p = 1005 \text{ KJ/kg.K}$$

$$\gamma = 1.4$$

$$R = 287$$

$$M_a = 114.399 \text{ Kg/sec}$$

$$\eta_{\text{poly}} = 0.94$$

Blade Design

Cascade measurements

In order to obtain information on the effect of different blade designs on air flow angles, pressure losses and energy transfer across blade rows, one must resort to cascade wind tunnels and cascade theory. Experimentation here is performed to ensure that the blade row satisfies its objectives. The first objective is to turn air through the required angles $(\beta_1 - \beta_2)$ for rotor and $(\alpha_3 - \alpha_2)$ for stator, with the angle $(\beta_1 - \beta_2)$ as a maximum as possible

to maximize the stage pressure ratio. The second objective is to achieve the diffusing process with optimum efficiency, i.e., with minimum loss of stagnation pressure.

Calculation of no. of blades

We determine the number of blade at all stage and the chord length at all radii for all station.

Details:

For rotor we use β_1 & β_2 and for stator we use α_2 & α_3 .

For Rotor

At mean section

$$\epsilon * = \beta_1 - \beta_2 \text{ We get s/c}$$

We assume,

$$C = h/3(\text{Equ.15}) \text{ for low pressure compressor}$$

$$\text{Then, } S = (S/C) * C (\text{Equ.16})$$

No. of blade = $(2\pi * r_m)/S$ (Equ.17) From experience for rotor number of blade is odd and for stator is even to avoid numbers with common multiples for the blades in successive rows to reduce the likelihood of introducing resonant forcing frequencies.

Where:

- Aspect ratio (h/c) is defined as height divided by vane or blade chord.

- C The chord.

- S the space between two blades.

For Stator:-

At mean section

$$\epsilon * = \Delta \alpha \text{ We get s/c}$$

$$T_s = T_{03} - \frac{C_a^2}{2C_p}$$

$$P_3 = P_{03} \left(\frac{T_3}{T_{03}} \right)^{\frac{\beta}{\beta-1}}$$

$$\rho_3 = \frac{P_3}{R * T_3}$$

$$M_{Tot.} = \rho_3 * A * C_{a3}$$

$$A = \frac{M_{Tot.}}{\rho_3 * C_{a3}}$$

$$A = 2 \pi * r_m * h_s$$

$$h_s = \frac{A}{2\pi * r_m}$$

Figure 9 shows variation of r_h and r_i with the compressor stages. Table 12 shows the calculated number of blades of each stage for HPC. Figure 10 shows variation of air density (kg/m^3) along the compressor stages.

Table 12: Calculated Number of blades of each stage for HPC

r_t (m)	r_h (m)	H (m)	C	S/C	S	N
0.342	0.267	0.075	0.037	1.7	0.063	30
0.336	0.274	0.062	0.031	1.7	0.053	36
0.357	0.279	0.078	0.039	1.7	0.066	29
0.331	0.282	0.049	0.024	1.7	0.041	46
0.324	0.285	0.039	0.019	1.7	0.032	60
0.321	0.288	0.033	0.016	1.7	0.027	70
0.319	0.290	0.029	0.014	1.7	0.024	79
0.318	0.292	0.026	0.013	1.7	0.022	86
0.316	0.293	0.023	0.011	1.7	0.018	106
0.315	0.294	0.021	0.010	2	0.02	95

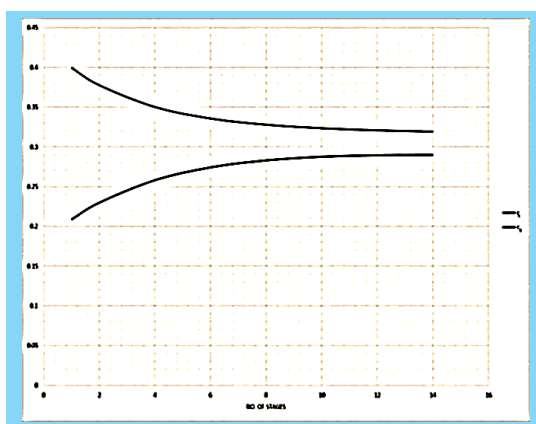


Figure 9: Variation of r_t and r_h with the compressor stages. The upper curve is r_t and the lower curve is r_h

We assume,

$$C = h/3 \text{ for low pressure compressor}$$

Then,

$$S = (S/C) * C$$

$$\text{No. of blade} = (2\pi * r) / s$$

From experience for rotor number of blade is odd and for stator is even to avoid numbers with common multiples for the blades in successive rows to reduce the likelihood of introducing resonant forcing frequencies

Where:

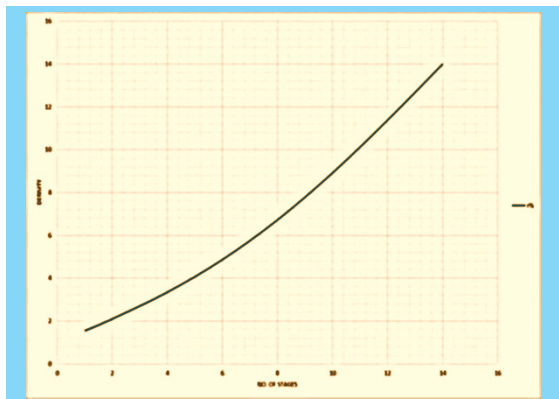


Figure 10: Variation of air density along the compressor stages

- Aspect ratio (h/c) is defined as height divided by vane or blade chord.
- C The chord.
- S the space between two blades.

2-D Performance Analysis (Takeoff)

Figure 11 shows Effect of bypass ratio on the specific thrust.

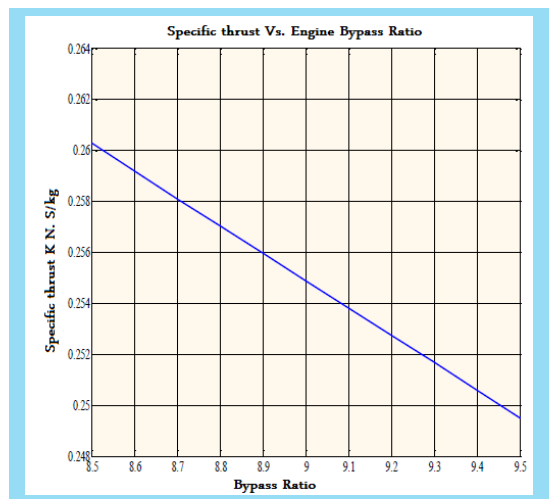


Figure 11: Effect of bypass ratio on the specific thrust

3-D Performance Analysis (Cruise Condition)

Figure 12 shows the effect of OPR on the thermal efficiency. Figure 13 shows the effect of both FPR and OPR on the overall efficiency.

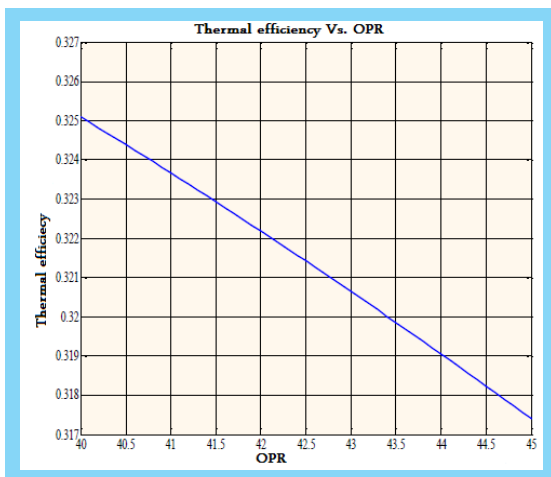


Figure 12: Effect of OPR on the thermal efficiency

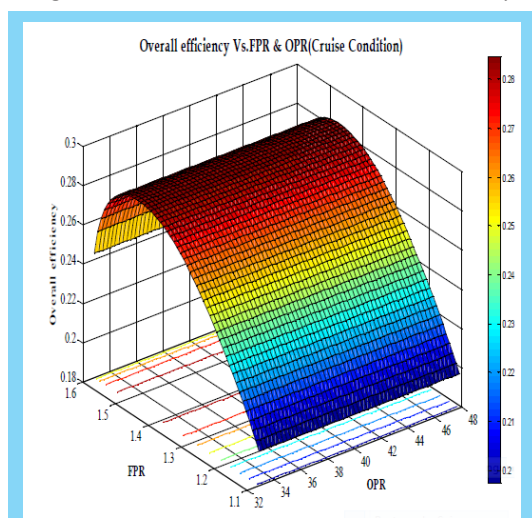


Figure 13: Effect of both FPR and OPR on the overall efficiency

Conclusion

The turbofan engine has a high thrust capability with low fuel consumption. From our study to the performance of one model of the turbofan engine we concluded that thrust force increases when the turbine inlet temperature increases but there is a metallurgical limitation. The thermal efficiency decreases when the overall pressure ratio of the engine increases. The specific thrust decreases when the bypass ratio increases. Finally, as the turbofan engines have many advantages, they are used the modern age in transportation and military aircrafts.

References

1. El-Sayed AF. Fundamentals of aircraft and rocket propulsion. Springer; 2016.
2. El-Sayed AF. Aircraft propulsion and gas turbine engines. CRC Press; 2017.
3. Boyce MP. Gas turbine engineering handbook. Elsevier; 2011.
4. Saravanamuttoo HIH, Rogers GFC, Cohen H. Gas turbine theory. Pearson Education; 2001.